Miniaturized High-Temperature Superconductor Microstrip Patch Antenna

Heinz Chaloupka, *Member*, *IEEE*, Norbert Klein, Michael Peiniger, Helmut Piel, Arndt Pischke, and Georg Splitt

Abstract—**This paper presents experimental as well as computational results for 2.4 GHz microstrip antennas which are miniaturized (total length, 6 mm) by both a new, "stepped impedance" patch shape and a relatively high substrate permittivity. The investigated antennas were fabricated from $YBa_2Cu_3O_{7-\delta}$ thin films epitaxially grown on single-crystalline $LaAlO_3$ substrates by pulsed excimer laser ablation or by high-pressure oxygen dc sputtering and, for comparison, from copper on the same substrate material. It is shown that the radiation efficiency of this antenna structure is only about 1% to 6% (depending on the substrate height) for copper at 77 K but is increased to values between 35% and 65% for HTS films. In the latter case, considerable improvements could be obtained if a substrate compatible with a high-temperature superconductor with a lower loss tangent were available. From experimental investigations of the power dependence of the antenna gain at 77 K, nonlinearities, especially a sharp drop at a current density of about $2 \cdot 10^6$ A/cm^2, were observed.**

I. Introduction

THE surface resistance of currently available epitaxial HTS thin films at 77 K and for frequencies below 10 GHz is lower by at least a factor of 100 than that of copper at the same temperature [1]. This allows microwave components for the lower frequency regime (0.1 to 10 GHz) to be miniaturized without a degradation of their relevant electrical properties [2].

In certain RF systems one is interested in a considerable reduction of the geometric size of antennas, e.g. for the case of small platforms or if several antennas have to be incorporated into a limited space. This requirement for miniaturization also arises if a VHF or a UHF antenna has to be part of an integrated receiver module because a conventional nonminiaturized antenna is often one order of magnitude larger than the remaining integrated semiconductor circuit.

Manuscript received October 25, 1990; revised February 15, 1991. This work was supported by the German Federal Minister for Research and Technology (BMFT) under Contract 13 N 5502.

H. Chaloupka, H. Piel, and A. Pischke are with the University of Wuppertal, D-5600 Wuppertal 1, Germany.

N. Klein was with University of Wuppertal, Wuppertal, Germany. He is now with Forschungszentrum KFA Jülich GmbH, D-5170 Jülich, Germany.

M. Peiniger is with Interatom GmbH, D-5060 Bergisch Gladbach, Germany.

G. Splitt is with DLR, D-8031 Weßling, Germany.

IEEE Log Number 9101133.

An antenna is referred to as electrically small if it can physically be bounded by a sphere of radius less than $\lambda_0/2\pi$, with λ_0 the free-space wavelength [3]. The radiation quality factor, Q_{rad}, of small antennas can be defined via the ratio of the mean energy, W, stored in the near field to the energy radiated during one period (power):

$$Q_{rad} = \omega W / P_{rad}. \tag{1}$$

Q_{rad} sharply increases if the geometric size, b, of an antenna is reduced to be "much less" than λ_0 [4], [5]. If a matching network is used together with the small antenna, it is in the following assumed to be part of the antenna, so that W in (1) also includes the mean energy stored within the matching circuit. Owing to losses in the conductors (P_c) and dielectric material (P_{diel}) the radiated power, P_{rad}, is less than the total power fed into the antenna. So the radiation efficiency becomes

$$\begin{aligned}\eta &= P_{rad}/(P_{rad} + P_c + P_{diel}) \\ &= 1/(1 + Q_{rad}/Q_c + Q_{rad}/Q_{diel})\end{aligned} \tag{2}$$

where Q_c and Q_{diel} are quality factors defined according to (1) but with P_{rad} replaced by P_c and P_{diel}, respectively. Equation (2) clearly indicates that a high value of Q_{rad} originating from a considerable antenna size reduction results in a "high sensitivity" of the radiation efficiency to the dissipation losses. The higher Q_{rad}, the lower the dissipation losses have to be in order to give a high efficiency. The allowed size reduction is restricted to a value b_{min}/λ_0 (according to $Q_{rad,max}$) if η is required to be larger than a minimum value, η_{min}. Increasing Q_c by replacing normal conductors by high-temperature superconductors (HTS's) and Q_{diel} by using low-loss-tangent dielectric material leads to a smaller antenna for the same efficiency [5]–[7]. If the antenna is with respect to its frequency response allowed to be modeled by a single resonant circuit, one obtains, for the half-power bandwidth in the case of a matched load [4],

$$\Delta f / f_0 = 2/(Q_{rad}\eta). \tag{3}$$

By reducing the dissipation losses in a given antenna structure (Q_{rad} fixed) the desired increase in η is connected with reduced frequency bandwidth.

The importance of the radiation efficiency for a receiving antenna follows from the consideration of the system noise temperature, T_{syst}, of a configuration consisting of an antenna (antenna noise temperature, T_A (external noise

0018-9480/91/0900-1513$01.00

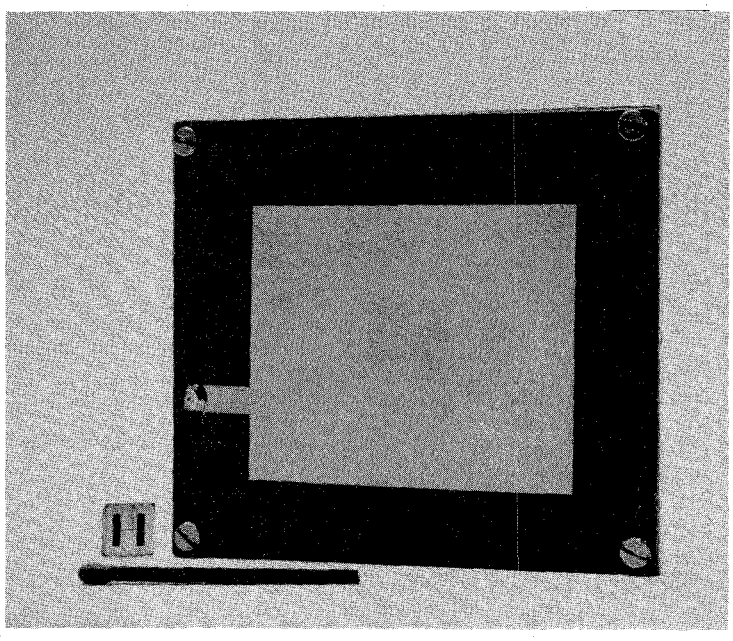

Fig. 1. Comparison of a conventional, normally conducting (*right*) and miniaturized HTC antenna (*left*) for 2.4 GHz. Substrate materials are RT-Duroid with $\epsilon_r = 2.2$ and $LaAlO_3$ with $\epsilon_r = 25$.

sources), radiation efficiency, η, and physical temperature, T) and an amplifier with effective noise temperature T_{ampl}:

$$T_{\text{syst}} = T_A + T_{\text{eff}} \quad \text{with} \quad T_{\text{eff}} = \frac{1-\eta}{\eta} T + \frac{1}{\eta} T_{\text{ampl}}. \quad (4)$$

From this equation the following conclusions can be made: (a) T_{eff} is largely increased if η becomes small. (b) Small values of T_{eff} are of interest if the external noise contributions represented by T_A are sufficiently small or are to be determined (radiometry).

In the case of a microstrip antenna the totally radiated power is divided into a (desired) space wave (P_{rad}) and an undesired surface wave contribution, P_{sw}, so that (2) has to be modified:

$$\eta = P_{\text{rad}} / (P_{\text{rad}} + P_c + P_{\text{diel}} + P_{\text{sw}}). \quad (5)$$

Since $P_{\text{sw}}/P_{\text{rad}}$ increases but $(P_c + P_{\text{diel}})/P_{\text{rad}}$ decreases with the substrate height, an optimum substrate thickness with respect to the radiation efficiency exists. For conventional rectangular patch antennas it is of the order of $0.005\lambda_0$ to $0.05\lambda_0$.

II. Principle

Conventional microstrip patch antennas are usually operated at resonance, which results at center frequency in a real input impedance at the feed point without the need for an additional matching network. As a consequence, the linear size of the patch is determined by the resonance condition. For a rectangular patch antenna the length has to be chosen to be about half a wavelength in material ($\lambda_g/2$). If this size has to be reduced without changing the rectangular shape of the patch, a substrate with higher permittivity, ϵ_r, is required. Rather than increasing ϵ_r, miniaturization can be obtained by employing a modified patch shape. It is well known that the total length, b, of a $\lambda_g/2$ transmission line resonator can be considerably reduced by using a "stepped-impedance" structure consisting of a high-characteristic-impedance (Z_1) line section of length $b-2d$ between two open-ended low-impedance (Z_2) line sections of length d (see Fig. 5). For $d = b/4$, from basic transmission line theory the total length, b, is determined by

$$\tan^2(\pi b / 2\lambda_g) = Z_2 / Z_1. \quad (6)$$

This consideration resulted in the patch shape shown in Fig. 1 (*left side*), which may be modeled very crudely as a stepped-impedance resonator. In a first size estimation a conventional rectangular patch antenna for 2.4 GHz would have a length of about $b = 42$ mm for RT-Duroid ($\epsilon_r = 2.2$) as substrate (Fig. 1, *right*) and of about $b = 12.5$ mm for $LaAlO_3$ with $\epsilon_r = 25$. If additionally the rectangular shape is replaced by an H shape (Fig. 5), one ends up with a total length of $b = 6$ mm. Thus, the miniaturization shown in Fig. 1 is due to both an increased permittivity and a change in the patch shape. To obtain the same miniaturization factor without changing the rectangular patch shape, a permittivity of about $\epsilon_r = 110$ would be required.

As an alternative to the "stepped-impedance patch antenna," the antenna may also be viewed as an end-loaded printed microstrip dipole.

For a rigorous design of the antenna geometry a moment-method-based computer code (see the Appendix) was employed. In this computation the extension of the substrate and ground plane is taken to be infinite. The result obtained for the current density distribution is given in Fig. 2, whereas Fig. 3 shows the computed far-field radiation pattern, indicating the fact that the

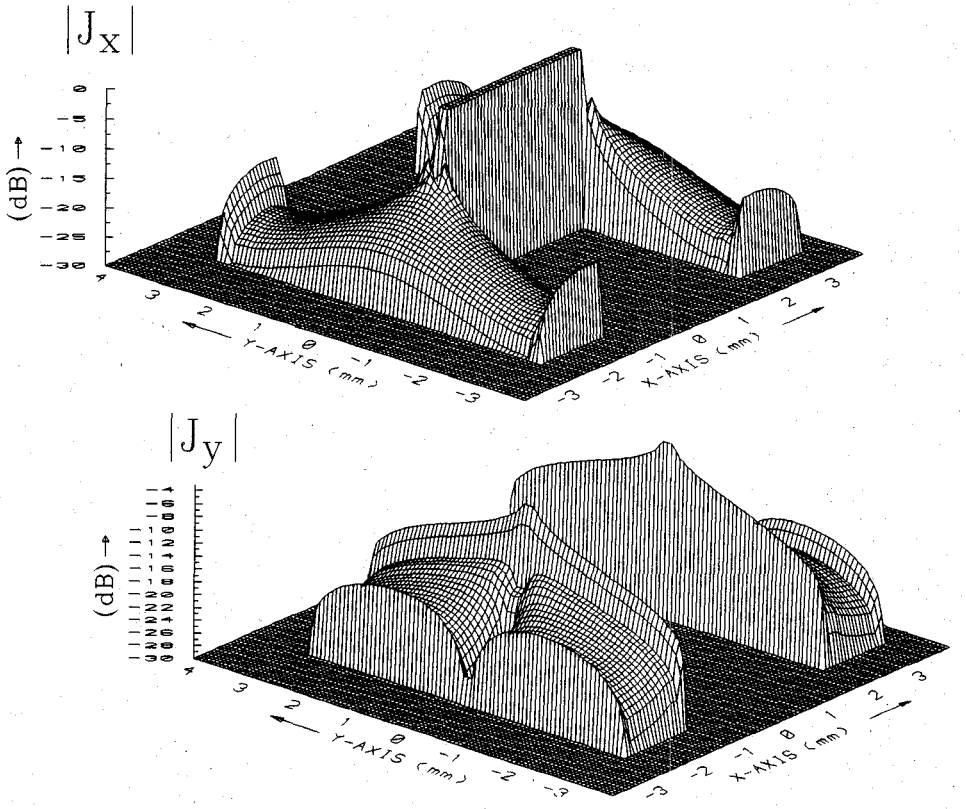

Fig. 2. Computed current density distribution on miniaturized patch antenna. Components J_x parallel and J_y perpendicular to small strip conductor.

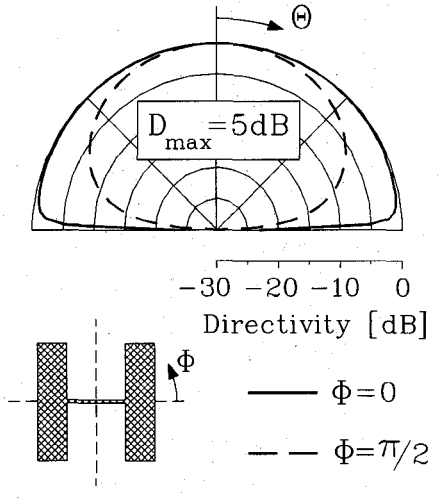

Fig. 3. Computed far-field radiation pattern in plane parallel (———) and perpendicular (– – –) to small strip conductor.

antenna radiates like a magnetic dipole oriented parallel to the substrate surface and perpendicular to the small conducting strip.

III. HTS Film, Substrate, and Antenna Configuration

The experimental results given in subsection IV-A are obtained with an antenna structure which was selected from three fabricated versions with respect to the power dependence of the antenna properties (see also Section V). All three versions used $YBa_2Cu_3O_{7-\delta}$ (short: YBCO) thin films epitaxially grown on single-crystalline ⟨100⟩ $LaAlO_3$ substrate with a thickness of 0.5 mm and a size of 10×10 mm^2. One of the films was deposited by pulsed excimer laser ablation [8] and two by a high-pressure oxygen dc sputtering technique [9]. Before the films were patterned by photolithography and chemical etching, the surface resistance, R_s, was measured by using the sample (substrate plus thin film) as an end plate of a cylindrical resonant copper cavity which can be operated at 86.3 GHz in the TE_{021} mode and at 86.9 GHz in the TE_{013} mode [10]. Fig. 4 shows the measured surface resistance as a function of temperature for the film produced by laser ablation, which was finally used for forming the patch of the antenna structure under investigation.

The effective surface resistance at 86.9 GHz and 77 K is approximately $R_{\text{eff}} = 60$ mΩ. This value is with respect to the film thickness of about 250 nm enhanced in comparison with the surface resistance for the (theoretical) case of infinite film thickness [11]. The latter can be estimated to be of the order of 30 mΩ, which is comparable to the best values presently available [1]. The quadratically scaled R_{eff} value at 2.4 GHz is $4.5\cdot10^{-5}$ Ω. This is about 130 times lower than the corresponding value ($6\cdot10^{-3}$ Ω) of high-purity copper at 77 K. The geometry of the complete antenna structure is shown in Fig. 5. In order to allow for variations of the coupling during the experiments, aperture coupling to an open-ended coaxial

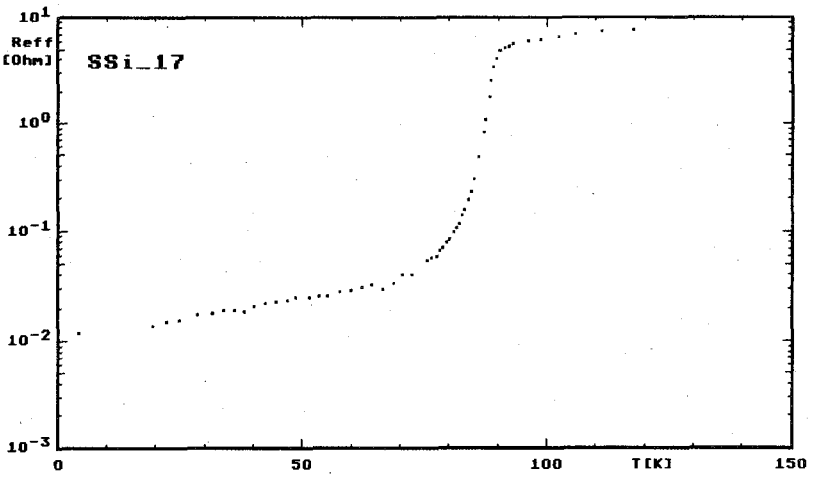

Fig. 4. Surface resistance R_s at 86.9 GHz as a function of temperature for the epitaxially grown YBCO thin film (laser ablation) which was used to build the miniaturized antenna.

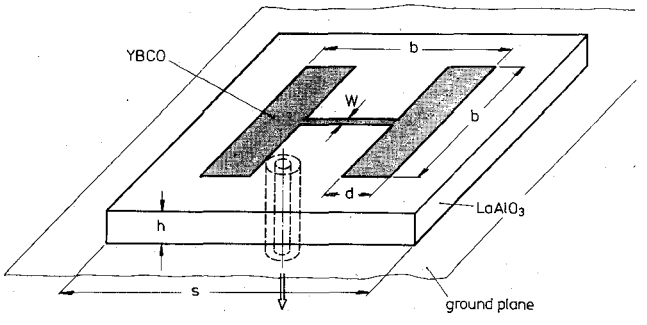

Fig. 5. Geometry of the miniaturized patch antenna ($b = 6$ mm, $d = 1.5$ mm, $w = 0.15$ mm, $h = 0.5$ and 1.0 mm, $s = 10$ mm).

feed line was utilized. The position of the inner conductor of the coaxial line can be changed to provide distances between 0 and 1 mm from the open end of the coaxial line to the lower plane of the substrate.

Three different configurations were used: The first has a total substrate height $h = 1$ mm, achieved by placing a 0.5-mm-thick substrate with an H-shaped YBCO conducting structure on top of a second 0.5-mm-thick substrate with a YBCO ground plane having a hole for coupling to the coaxial line. The second is the same as the first, but without a YBCO ground plane on the second substrate. The configuration therefore presents a total substrate height $h = 1$ mm with superconducting patch structure, but normal conducting ground plane. The third configuration has a total substrate height $h = 0.5$ mm with a superconducting patch structure and a normal conducting ground plane, achieved by using only one substrate.

IV. Efficiency

A. Experimental Results

In order to investigate the microwave properties of the miniaturized patch antennas in the temperature range between 70 K and 300 K they were mounted on top of a cold finger (Fig. 6) located in an evacuated glass Dewar (Fig. 7). The miniaturized antenna was used as a transmitting antenna in a link about 1 m long with a wide-band ridged waveguide horn as the receiving antenna. All measurements have been made with an HP 8752A vector network analyzer. The result of a transmission experiment with respect to the temperature dependence is shown in Fig. 8. The coupling to the HTS antenna (YBCO patch, ground plane made from copper, substrate height $h =$ 1 mm) was adjusted to provide zero reflection ($|S_{11}| = 0$) at $T = 70$ K. It is found that the quantity $P_{\text{rad}}(T)/P_{\text{rad,max}} = |S_{21}|^2/|S_{21}|^2_{\text{max}}$ decreases slightly if the antenna is warmed up to 80 K but drops very sharply for $T > 83$ K. Note that this sharp drop is due to both a decreasing

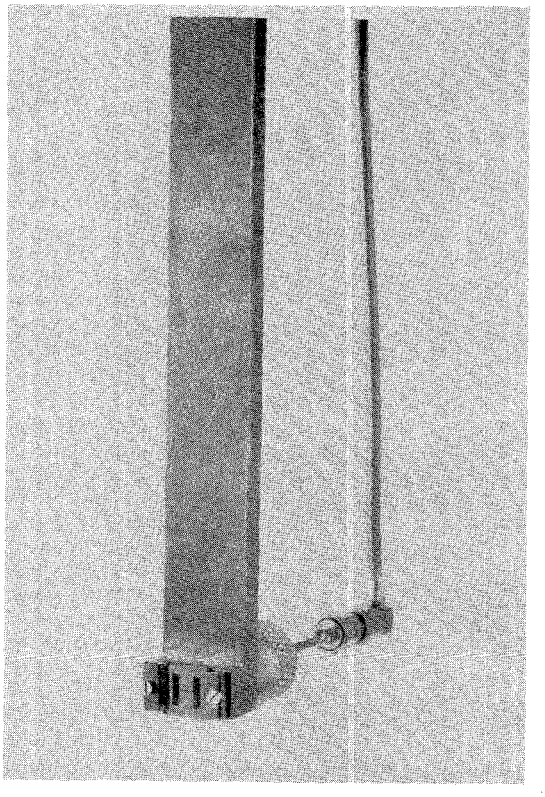

Fig. 6. Miniaturized HTS antenna mounted on top of a cold finger.

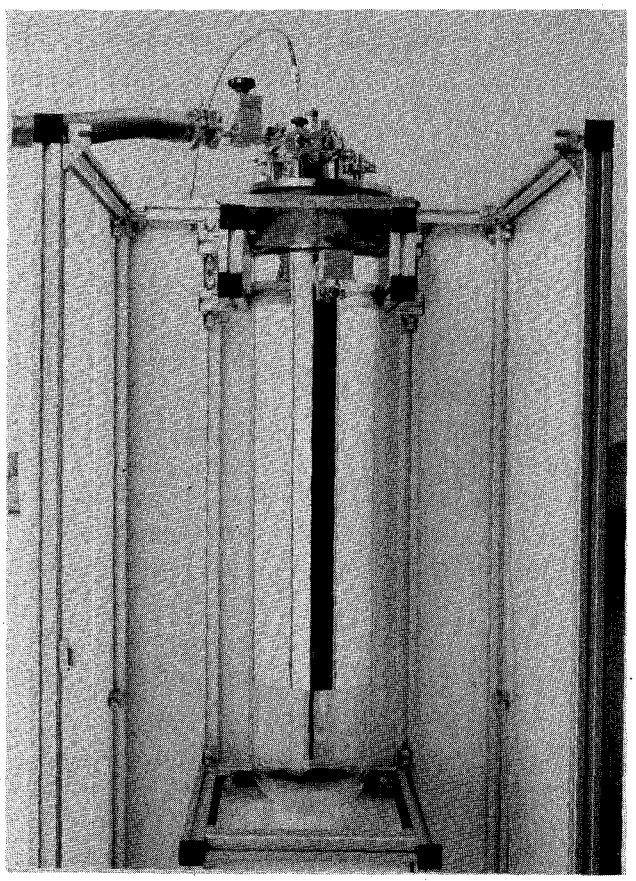

Fig. 7. Cryostat for measuring the properties of HTS antennas from $T = 70$ to 300 K.

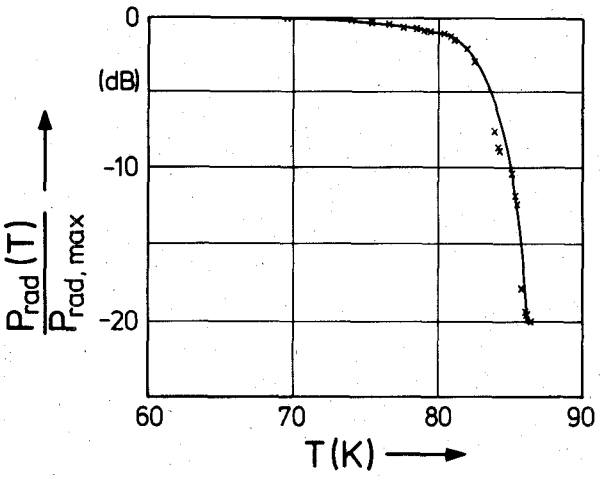

Fig. 8. Measured temperature dependence of the radiated power (HTS patch, Cu ground plane, $h = 1$ mm).

radiation efficiency (increasing conductor losses) and an increasing reflection coefficient $|S_{11}|$ at the antenna port. The half-power bandwidth at 77 K was about 3 MHz at a center frequency of 2.45 GHz.

The experimental determination of the radiation efficiency was performed by using the method proposed by Wheeler [12]. It is based on the idea of removing experimentally the radiated power by enclosing the antenna by a "radiation shield" (closed metallic box) with a size of the order of $\lambda_0/2\pi$. It should be mentioned that the shape and size of the box turned out experimentally not to be critical. By measuring the reflection coefficient S_{11} at the center frequency with and without the radiation shield and determining the corresponding values of the input resistance R^{w} and R^{wo}, the efficiency is obtained via

$$\eta = 1 - R^{w}/R^{wo}.$$

In order to avoid large errors, the coupling coefficient to the antennas should not be too far from its critical value ($|S_{11}| = 0$). The Wheeler method was utilized to determine η for HTS antennas (ground plane alternatively made from copper or HTS) with substrate thicknesses $h =$ 0.5 mm and 1.0 mm. Since the radiation coupling shown in Fig. 5 does not make it possible to realize strong coupling to the antenna, the method turned out to be not practicable in the case of a miniaturized antenna with a copper patch ("low" quality factor and therefore strong coupling required for $|S_{11}| \approx 0$). Furthermore because of the low efficiency, and therefore $R^{w} \approx R^{wo}$, large errors in η would result from the Wheeler method. The efficiency of the copper antennas was therefore evaluated from the ratio of the received power for the copper antenna (P_r^{Cu}) to the power for the HTS antenna (P_r^{HTS}).

Since replacing YBCO with copper does not significantly change the spatial distribution of the current density (except for the magnitude) at the patch, the directivity of the HTS and copper antennas can be assumed to be identical at all angles. Since furthermore the same receiving antenna and measurement configuration (distances between antennas, etc.) is used for both measurements, the directivity of the antenna under test, the properties of the receiving antenna, and the antenna distance cancel if the Friis transmission formula is used to derive the ratio of P_r^{Cu}/P_r^{HTS}. The resulting equation,

$$\frac{P_r^{Cu}}{P_r^{HTS}} = \frac{|S_{21}^{Cu}|^2}{|S_{21}^{HTS}|^2} = \frac{\eta^{Cu}\left(1-|S_{11}^{Cu}|^2\right)}{\eta^{HTS}\left(1-|S_{11}^{HTS}|^2\right)}$$

can be rewritten to solve for the efficiency, η^{Cu}, of the copper antenna as a function of the efficiency, η^{HTS}, of the YBCO antenna which was determined by Wheeler's method (see above).

Table I shows the experimentally obtained results. In the case of the HTS antennas the input power was decreased to a level where no power dependence of $|S_{11}|$ could be observed. The results in the table are therefore "low-power" results. The power dependence for a higher power level is discussed separately in Section V. The given range of results in Table I corresponds to measurements which have been repeated several times and with different levels of strong coupling to the antennas.

The measured far-field radiation pattern showed good agreement with the computed results from Fig. 3, except for some deviations (oscillating with angle) of less than 0.5 dB for $\Theta = \pi/2$ (see Fig. 3) which are due to the influence of the surrounding cryostat (see Fig. 7).

TABLE I
EXPERIMENTAL RESULTS FOR THE RADIATION EFFICIENCY (IN PERCENT)

Substrate Height	Patch: YBCO Ground Plane: YBCO (77 K)	Patch: YBCO Ground Plane: Cu (77 K)	Patch: Cu Ground Plane: Cu (77 K)	Patch: Cu Ground Plane: Cu (300 K)
$h = 0.5$ mm	35–48	35–45	1.5–3	0.8–1.5
$h = 1$ mm	55–65	55–65	4–6	1–3

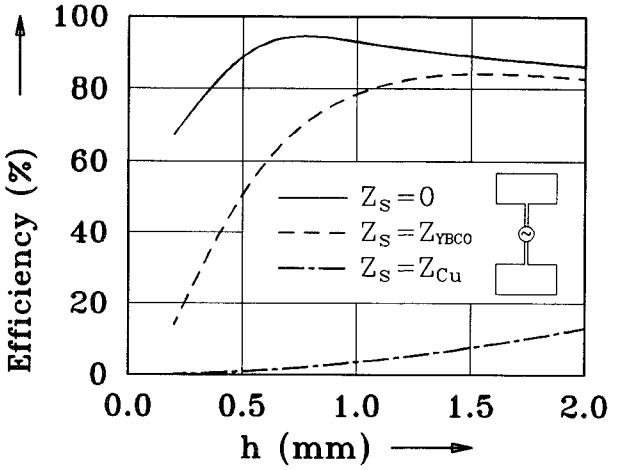

Fig. 9. Computed efficiency as a function of substrate height h for ideal conductors, copper at 77 K, and YBCO at 77 K ($\tan\delta = 10^{-5}$).

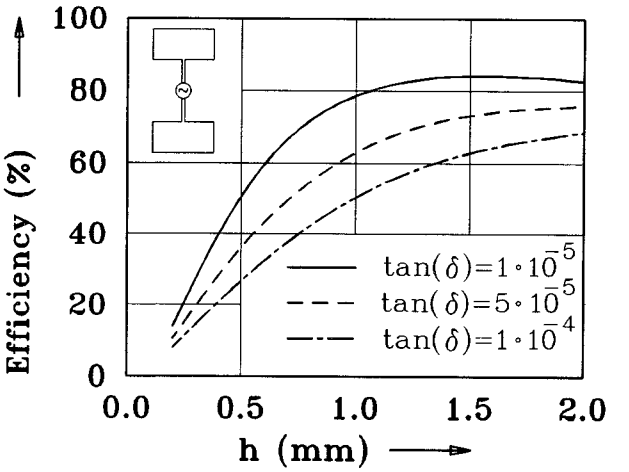

Fig. 10. Computed efficiency as a function of substrate height h for YBCO structure at 77 K for different loss tangents of the substrate.

B. Numerical Results

The miniaturized antenna structure of Fig. 5 was also investigated theoretically. This was done by solving the electromagnetic boundary value problem (patch structure at a transverse infinite substrate and ground plane, direct excitement by a voltage gap generator in the small conductor strip instead of the coaxial coupling shown in Fig. 5) by means of the moment method (see the Appendix). From the solution (current density distribution, Fig. 2, and the radiated field, Fig. 3) numerical values for the efficiency have been derived for a large variety of material parameters. In Fig. 9 the results for the efficiency as a function of the substrate height, h, are shown for an ideal conductor ($Z_s = 0$), YBCO at 77 K with $Z_s = (4.5 + j500)\cdot 10^{-5}\ \Omega$, and Cu at 77 K with $Z_s = 6\cdot 10^{-3}\ (1+j)\ \Omega$. The substrate is in this case modeled by $\epsilon_r = 25$ and $\tan\delta = 10^{-5}$. To demonstrate the effect of dielectric losses on the radiation efficiency, Fig. 10 compares substrates with $\epsilon_r = 25$ but different loss tangents. The conductors are taken to be YBCO at 77 K (see above).

C. Discussion

The numerical results (Figs. 9 and 10, and a number of results not shown here) are in fairly good agreement with the experimental results (Table I) for YBCO at 77 K if the loss tangent of the substrate is chosen to be about $0.5\cdot 10^{-4}$ (Fig. 10). Also for copper at 77 K, good agreement between numerical and experimental data is obtained. In the latter case variations of $\tan\delta$ in the regime $\leqslant 5\cdot 10^{-4}$ have no relevant influence on η.

In order to allow a basic discussion of the influence of the substrate height, h, as well as the surface resistance, R_s, and the loss tangent, $\tan\delta$, on the radiation efficiency, η, an approximation formula was derived by assuming $P_c/P_{\text{rad}} \sim R_s/h^2$ and $P_{\text{diel}}/P_{\text{rad}} \sim \tan\delta/h$ and determining the numerical coefficients by a least-squares fit to the numerical results obtained with the moment method:

$$\eta = \eta(h, \tan\delta, R_s) \sim \frac{1}{1 + \dfrac{0.8}{h}\dfrac{\tan\delta}{10^{-4}} + \dfrac{4.5}{h^2}R_s + F_{\text{sw}}(h)}. \tag{7}$$

In this formula h is the substrate height in mm and R_s the surface resistance in mΩ. $F_{\text{sw}}(h)$ is a function which accounts for the surface wave contribution. For a substrate height of less than 1.25 mm and $R_s \geqslant 10^{-2}$ mΩ, the numerical data for η obtained with the moment method are well approximated by (7) if the surface wave contribution is neglected ($F_{\text{sw}} = 0$). It can be concluded from (7) that the conductor losses exceed the dielectric losses if $R_s/\text{m}\Omega > 0.18\ h/\text{mm}\cdot\tan\delta/10^{-4}$.

In the case of a normal conducting patch structure, $h \leqslant 1.25$ mm, and $\tan\delta \leqslant 2\cdot 10^{-4}$, conductor losses are at least one order of magnitude higher than the dielectric losses. In the case of an HTS with $R_s = 4.5\cdot 10^{-2}$ mΩ the substrate losses exceed the conductor losses if $\tan\delta \geqslant 0.25\cdot 10^{-4}/(h/\text{mm})$.

As discussed above, both the higher permittivity of the substrate and the stepped impedance design (H shape) made it possible to reduce the linear size as well as the

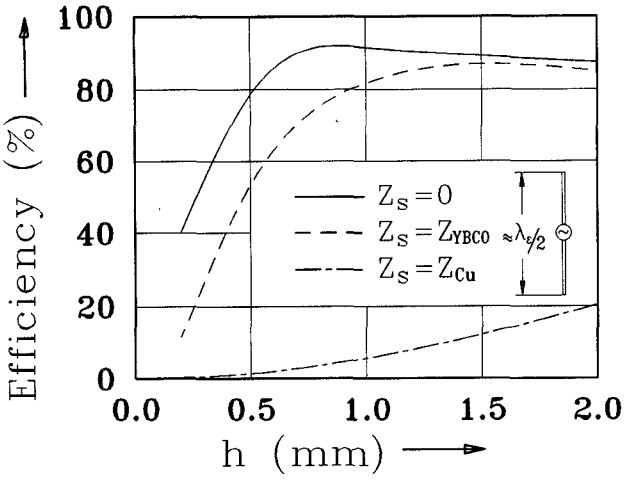

Fig. 11. Computed efficiency as a function of substrate height h for a printed microstrip dipole (copper and YBCO at 77 K and ideal conductor, $\epsilon_r = 25$, $\tan\delta = 10^{-5}$). The conducting surface area (length 12 mm, width 1.5 mm) is chosen to be equal to the surface area of the H-shaped antenna under consideration (see Figs. 5 and 9).

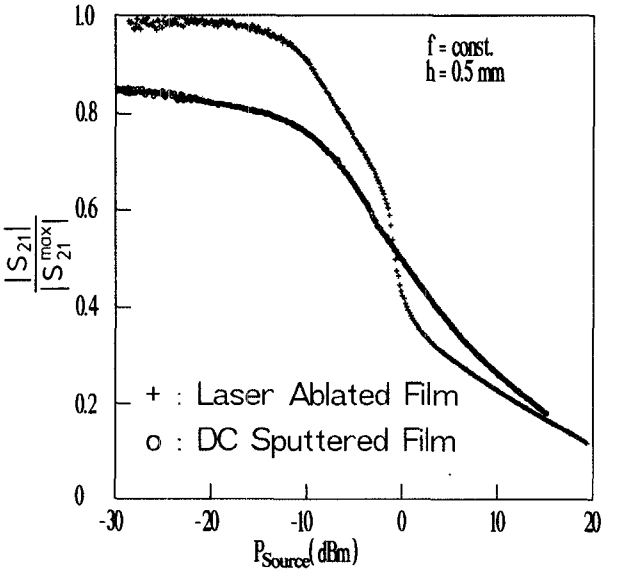

Fig. 12. Measured transmission factor (relative) as a function of input power level for constant frequency (YBCO) patch, Cu ground plane, $h = 0.5$ mm) at 77 K.

surface area occupied by the plane conductor. In order to demonstrate the effect of the H shape separately from the increase in ϵ_r, a comparison is made with a printed microstrip dipole.

This dipole is assumed to have the same ϵ_r value for the substrate and to occupy the same conducting area, but for the given frequency of operation, as a consequence of its rectangular patch shape, is twice as long as the H-shaped antenna. Fig. 11 shows the computed efficiency for this printed microstrip dipole (length $b = 12$ mm, width $w = 1.5$ mm) as a function of the substrate height, h, for copper at 77 K, YBCO at 77 K, and (theoretically) ideal conductors. The values of ϵ_r and $\tan\delta$ are taken to be the same as in Fig. 9. By comparing Fig. 11 with Fig. 9, the following conclusions can be drawn:

a) In the normal conducting case the reduced length (factor 0.5) of the H-shaped antenna is achieved at the cost of an efficiency reduction of the order of 0.5 to 0.7.
b) However, the efficiency of the approximately 12 mm long printed microstrip dipole in the normal conducting case even at 77 K is rather low (7% to 20% for h between 1 and 2 mm).
c) By replacing the normal conducting printed dipole by an HTS dipole, its efficiency is also highly improved, but not to a considerably higher amount than in the case of the much shorter H-shaped antenna.

V. Observation of Nonlinearities

The power dependence of the microwave properties can be studied in, e.g., a transmission experiment with the HTS antenna as transmitting antenna and the coupling chosen to give zero reflection for low input power, P_{source}. If this power is increased a nonlinear behavior resulting in a decreasing transmission coefficient, $|S_{21}|$, can be observed (see Fig. 12). A very crude estimate of the current density in the small strip conductor of the antenna can be derived if one assumes the conductor losses to be concentrated within a small strip conductor of width $w = 0.15$ mm and length $(b - 2d) = 3$mm (see Fig. 5):

$$P_c \approx 0.5|J|^2 w(b-2d)R_s\lambda. \tag{8}$$

Here $\lambda \approx 250$ nm is the penetration depth and $|J|$ is taken to be constant on the surface of the strip conductor. The conductor losses can from (5) with $P_{sw} \approx 0$ and (7) be related to P_{source} by

$$P_c \approx (1-|S_{11}|^2)P_{source}\frac{1-\eta}{1+2000h\cdot\tan\delta/R_s}. \tag{9}$$

This crude estimation of the relationship between current density, J, in the small strip conductor and P_{source} given by (8) and (9) is in good agreement with the corresponding data obtained by the numerical method described in the Appendix.

The antenna built from a laser ablated film behaves according to Fig. 12 in nearly linear fashion up to $P_{source} \approx -15$ dBm ($J \approx 0.5\cdot 10^6$ A/cm^2) but shows a first relatively slowly decreasing behavior of the transmission coefficient in the range between -15 to 0 dBm. At about 0 dBm ($J \approx 2\cdot 10^6$ A/cm^2) a remarkably sharp falloff can be observed. For higher power level again a relatively slow decrease can be seen. The antenna built from a dc sputtered film has a lower low-power efficiency (surface resistance, $7.5\cdot 10^{-5}$ Ω) and the falloff of $|S_{21}|$ starts at a lower power level than for the laser ablated film. Furthermore, the sharp falloff observed for the laser ablated film is not seen for the dc sputtered film.

VI. Conclusions

The geometric size of resonant planar antennas in the VHF or UHF regime can be considerably reduced by

TABLE II
MODIFICATION OF GREEN'S FUNCTION

a) modeling of the impedance ground-plane:

$$\tilde{G}^{(1,1)}_{\varepsilon,\mu} = \left[Y^{(1)}_{\varepsilon,\mu} \cdot Z_{sg} + \tanh(h_1\gamma_1)\right] \cdot D^{-1}_{\varepsilon,\mu}$$

$$D_{\varepsilon,\mu} = \left[Y^{(1)}_{\varepsilon,\mu} \cdot Z_{sg} + \tanh(h_1\gamma_1)\right] \cdot Y^{(0)}_{\varepsilon,\mu} + Y^{(1)2}_{\varepsilon,\mu} \cdot Z_{sg} \cdot \tanh(h_1\gamma_1) + Y^{(1)}_{\varepsilon,\mu}$$

$$\gamma_i = \sqrt{k_x^2 + k_y^2 - \varepsilon_i k_0^2}\ ; \quad Y^{(i)}_{\varepsilon} = \frac{j\varepsilon_i k_0}{\gamma_i Z_0}\ ; \quad Y^{(i)}_{\mu} = \frac{\gamma_i}{j\mu_i k_0 Z_0}$$

b) modeling of the impedance surface of the structure:

$$\tilde{G}^{(nn')}_{\varepsilon,\mu} \Rightarrow \tilde{G}^{(nn')}_{\varepsilon,\mu} - Z_s\,\delta_{nn'}$$

means of a modified "patch shape" including small-width transmission line sections. Owing to both the increased radiation quality factor and increased losses in the small strip conductors, this miniaturization results in a very low (a few percent) value of the radiation efficiency in the case of normal conducting antenna structures. The utilization of HTS thin films together with low-loss substrates allows the radiation efficiency to be increased to values which are typical for the much larger normal conducting conventional patch antennas. This improvement is obtained by the cost of a reduced frequency bandwidth. Furthermore, high-power nonlinearities in high-Q structures may limit their applicability to receiving antennas.

As a generalization of the obtained results, it can be concluded that more complex antenna structures (e.g. with matching network) including small-width transmission line sections can be realized without a reduction in radiation efficiency if the normal conducting structures are replaced by epitaxial HTS films at 77 K.

APPENDIX

In the numerical calculation of the current distribution (Fig. 2), the radiation pattern (Fig. 3), and the efficiency (Figs. 9, 10, and 11), the computer code described in [13] and [14] has been used. For taking into account both the surface impedance of the ground plane and the antenna structure ("patch"), the following modifications of the Green's function became necessary. The surface impedance of the ground plane is incorporated by replacing the short cut in the matrix model of the dielectric layer [13] by a corresponding impedance Z_{sg} (Table II). Modeling of the superconducting antenna structure is done by formulating the impedance boundary condition ($E = Z_s J$) [15]–[17] instead of the boundary condition for an ideal electrical conductor ($E_t = 0$). This procedure results in a very simple modification of the Green's function [16].

ACKNOWLEDGMENT

The authors would like to thank their colleagues G. Daalmans, G. Gieres, and L. Schultz from Siemens AG and U. Poppe and K. Urban from KfA Jülich for providing high-quality thin films and performing the structural work. Experimental and technological contributions by M. Jeck and B. Mönter are also gratefully acknowledged.

REFERENCES

[1] H. Piel and G. Müller, "The microwave surface impedance of high-T_c superconductors," *IEEE Trans.Magn.*, vol. 27, p. 854, 1991.
[2] H. Chaloupka, "High-temperature superconductors—A material for miniaturized or high-performance microwave components," *Frequenz*, vol. 44, no. 5, pp. 141–144, May 1990.
[3] F. Fujimoto, A. Henderson, K. Hirasawa and J. R. James, *Small Antennas*. Letchworth, U.K.: Research Studies Press, 1987.
[4] R. C. Hansen, "Fundamental limitations in antennas," *Proc. IEEE*, vol. 69, pp. 170–182, Feb. 1981.
[5] R. J. Dinger and D. J. White, "The radiation efficiency of a small dipole antenna made from a high-temperature superconductor," in *IEEE Antennas Propagat. Int. Symp. Dig.* (Dallas), 1990, pp. 724–727.
[6] G. B. Walker and C. R. Haden, "Superconducting antennas," *J. Appl. Phys.*, vol. 40, no. 5, pp. 2035–2039, 1969.
[7] R. C. Hansen, "Superconducting antennas," *IEEE Trans. Aerosp. Electron. Syst.*, vol. 26, pp. 345–355, Mar. 1990.
[8] B. Roas, L. Schultz, and G. Endres, "Epitaxial growth of $YBa_2Cu_3O_{7-x}$ thin films by a laser evaporation process," *Appl. Phys. Lett.*, vol. 53, pp. 1557–1559, Oct. 1988.
[9] U. Poppe *et al.*, "Epitaxial multilayers of $YBa_2Cu_3O_7$ and $PrBa_2Cu_3O_7$ as a possible basis for superconducting electronic devices," *Solid State Commun.*, vol. 71, pp. 569–572, July 1989.
[10] N. Klein *et al.*, "Millimeter wave surface resistance of epitaxially grown $YBa_2Cu_3O_{7-x}$ thin films," *Appl. Phys. Lett.*, vol. 54, pp. 757–759, Feb. 1989.
[11] N. Klein, H. Chaloupka, G. Müller, S. Orbach, and H. Piel, "The effective microwave surface impedance of high-T_c thin films," *J. Appl. Phys.*, vol. 67, no. 11, pp. 6940–6945, June 1990.
[12] H. A. Wheeler, "The radiansphere around a small antenna," *Proc. IRE*, vol. 47, pp. 1325–1331, Aug. 1959.
[13] G. Splitt, "Rectangular electromagnetically coupled microstrip antennas in multilayered structures," in *Proc. 18th European Microwave Conf.*, (Stockholm), Sept. 1988, pp. 1043–1048.
[14] G. Splitt, "A rapid method of arbitrary microstrip structures using the FFT-algorithm," in *Proc. 20th European Microwave Conf.* (Budapest), Sept. 1990, pp. 1481–1486.
[15] J. R. Mosig and F. E. Gardiol, "Ohmic losses, dielectric losses and surface waves effects in microstrip antennas," in *Dig. URSI Int. Symp. Electromagn. Theory* (Spain), pp. 425–428, 1983.
[16] J. M. Pond, C. M. Krowne, and W. L. Carter, "On the application of complex resistive boundary conditions to model transmission lines consisting of very thin superconductors," *IEEE Trans. Microwave Theory Tech.*, vol. 37, pp. 181–190, Jan. 1989.
[17] T. B. A. Senior, "Impedance boundary conditions for imperfectly conducting surfaces," *Appl. Sci. Res.*, vol. 8, pp. 418–436, 1960.

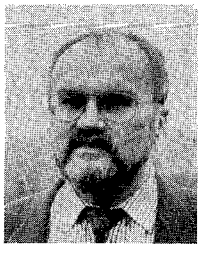

Heinz Chaloupka (S'68–M'69) received the Dipl.-Ing. degree from the Technical University Darmstadt in 1969 and the Dr.-Ing. degree in electrical engineering from the University of Bochum, Germany, in 1975.

From 1969 to 1975 he worked as a Research Assistant at the University of Bochum on electromagnetic theory and numerical methods for solving field problems. From 1976 to 1983 he was a Senior Research Engineer there conducting research on direct and inverse scattering problems, imaging with electromagnetic waves, and industrial applications of microwave, techniques. Since 1983, he has been a Professor of Microwave Techniques at the University of Wuppertal, Germany. His current research activities include microwave applications of high-temperature superconductors as well as modeling and reconstruction in electromagnetic remote sensing problems.

Dr. Chaloupka is a Member of Commission B of the International Union of Radio Science (URSI) and of a number of IEEE societies. He is currently chairman of the Radio Frequency Section within the ITG (Germany).

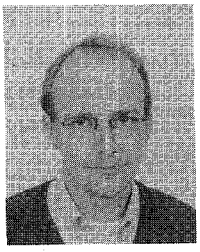

Norbert Klein was born in Wuppertal, Federal Republic of Germany, on May 30, 1959. He received a diploma in physics in 1985 and the Ph.D. degree in 1989, both from the Bergische Universität Wuppertal. At Wuppertal he worked first on superconducting niobium and Nb_3Sn millimeter-wave cavity resonators and then on Fabry–Perot-type open resonators. Since high-temperature superconductors were discovered, in 1986, he has been engaged in the investigation of the microwave surface impedance of high-T_c thin films.

Since September 1990 Dr. Klein has been head of a group at Forschungszentrum Jülich, FRG, working on the preparation of high-T_c thin films and the exploration of their microwave properties.

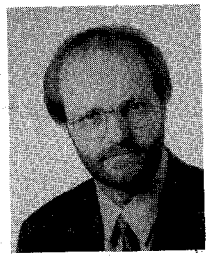

Michael Peiniger was born in Wuppertal, Federal Republic of Germany, on March 22, 1957. He received a physics diploma and the Ph.D. degree from the University of Wuppertal, FRG, in 1983 and 1989, respectively.

While at the University of Wuppertal he did research on RF superconductivity. Beginning in 1985, he worked on the transfer of superconducting accelerator cavity technology to industry. In 1987 he joined the Accelerator and Magnet Technology Division of Interatom GmbH, Bergisch Gladbach, FRG, where he has been working on accelerator cavities. Since 1989 he has been head of the accelerator technology group and is responsible for accelerator, RF, and cryogenic components and systems.

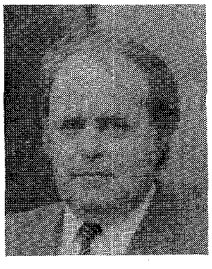

Helmut Piel received the Dr. rer. nat. degree in physics from the University of Bonn, Germany, in 1966. From 1965 to 1970 he was a Research Assistant in the Physics Department of the Bonn University.

After a two-year fellowship for experimental research work on deep inelastic electron nucleon scattering at the Stanford Linear Accelerator Center, in 1970/71, he returned to Bonn University, where he started a new research field on RF superconductivity and accelerator physics. After his "Habilitation," in 1973, he became a Full Professor at the new University of Wuppertal, Germany. His primary research work since 1972 has focused on the study of superconductivity materials in time-dependent electromagnetic fields with the goal of applying superconductivity cavities in high-energy accelerators and paving the way for their use in experimental physics and microwave technology. In 1979 he has spent a sabbatical year at CERN. Since 1986 he has been a Distinguished Visiting Professor at the College of William and Mary, Williamsburg, VA. In 1986 he received a prize for achievement in accelerator physics and technology awarded by the US Particle Accelerator School.

Dr. Piel was a Member of the Scientific Council of DESY, a Scientific Advisor of the Director General of CERN, and a Member of the National Advisory Board of CEBAF.

Arndt Pischke was born in Essen, Germany, in 1962. He received the Dipl.-Ing. degree in electrical engineering from the University of Wuppertal, Germany, in 1989.

Since then, he has been working as a Research Assistant in the Department of Microwave Techniques at the University of Wuppertal. He is engaged in the microwave application of high-temperature superconductors, particularly in the design of electrically small superconducting antennas.

Georg Splitt was born in Dortmund, Germany, in August 1956. He received the Dipl.-Ing. and the Ph.D. degree in electrical engineering from the University of Wuppertal in 1985 and 1991, respectively.

Since 1985 he has been working at DLR, the German Aerospace Research Establishment, in Oberpfaffenhofen, where he is responsible for the design, construction, and testing of antenna systems for radar and communication applications.

His current research interests cover the use of numerical methods for designing and predicting antenna behavior. In this connection he received the Microwave Prize at the European Microwave Symposium in Stockholm in 1988.